MULTI-SCALE TENSOR VECTOR FIELD ACTIVE CONTOUR

Abhishek Kumar, Alexander Wong, Paul Fieguth, and David A. Clausi

Department of Systems Design Engineering
University of Waterloo
Waterloo, Canada

ABSTRACT

Two major challenges faced in active contours are poor capture range and high sensitivity towards noise. Recently, the concept of tensor vector convolution (TVF) was introduced and shown to be promising in handling these challenges. However, in the presence of high noise levels, TVF may have difficulty in converging to the desired object boundary, particularly if the distance is great between the initial contour and the object boundary. To tackle this challenge, the concept of a multi-scale tensor vector field (MTVF) active contour is introduced to further reduce noise sensitivity. Comparing the performance of MTVF with multi-scale gradient vector field and multi-scale vector field convolution demonstrates that MTVF is more resilient to high noise levels as well as significantly reducing computation time.

Index Terms— Active Contour, Segmentation, Tensor Vector Field, Multi-scale tensor vector field, multi-scale active contour.

1. INTRODUCTION

First introduced by Kass et.al. [1], parametric active contours are capable of handling irregular shapes by implicitly handling object shapes using image and structural priors. Active contours find their application in many computer vision problems such as medical image analysis, object tracking, and object detection.

In active contours, an initial contour is initialized close to the boundary of object, either automatically or manually. The contour then changes iteratively via the minimization of an energy function [1], designed in such a way that in the ideal case the contour finds its minimum energy around the boundary of the object. The energy function consists of two components: i) the internal energy, and ii) the external energy. The internal energy represents the prior model, penalizing the contour from taking on an unexpected shape, while the external energy drives the contour towards the boundary of the object.

Geomatics for Informed Decisions (GEOIDE) and Discovery Grants, both funded by Canada's Natural Science and Engineering Research Council (NSERC), as well as Ontario Centers of Excellence (OCE) are thanked for project funding.

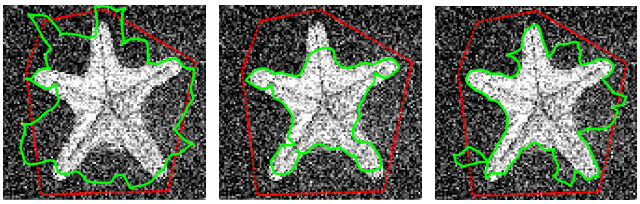

(a) GVF [2] (b) MGVF [3] (c) TVF [4]

Figure 1: Active contour results, green, for existing methods on starfish image (PSNR 14.2), given the initialization shown in red. We observe that high noise levels lead to a poor convergence of the contour.

Being an iterative optimization problem, the main challenge in selecting an energy function is to design it in such a way that it

- converges to the object boundary even if the contour is initialized far from the object boundary, i.e., improving the capture range), and
- does not get stuck in local minima due to the presence of noise or other artifacts, i.e., improving noise robustness.

There have been several efforts to tackle these two challenges. Several previous works were motivated by natural forces such as gravitation [5] and electrostatics [6]. The gradient vector field (GVF) [2] was proposed to improve capture range and to handle concave object boundaries. The active contour driven by GVF has indeed been found to handle capture range very effectively and it is able to diffuse the field towards and into concave boundaries, however the field is easily influenced by noise.

The vector field convolution (VFC) [7] external field has similar been shown to provide good results in term of noise handling properties and capture range into concave surfaces. Though more effective than GVF, VFC makes only limited use of structural information of the object boundary, and therefore has limited success in tackling noise. To address this issue, the tensor vector field (TVF) [4] was introduced and showed that a better utilization of structural information can significantly improve noise robustness.

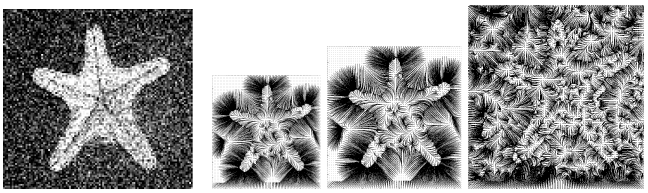

(a) Noisy Image (b) MTVF_2 (c) MTVF_1 (d) MTVF_0

Figure 2: Streamline of MTVF for a Gaussian noise contaminated starfish image (Fig. 6a) at 14.2 dB for three different resolution levels (not shown in same proportion). In streamline images, a higher consistency and density of dark regions towards the object boundary promises a better convergence of the active contour.

Though these methods of active contours have improved significantly over the traditional approaches, they still face issues when dealing with high noise levels (Fig. 1). More than a decade ago [8] had shown that multi-resolution active contours can help reduce noise sensitivity, as well as improve capture range and promote faster convergence. More recently, [3] introduced the concept of multi-scale GVF (MGVF) for effective mass segmentation in digital mammography. Motivated by these works, in this paper we introduce the concept of a multi-scale tensor vector field (MTVF) for active contours in order to handle high noise levels. Experiments show that MTVF can provide significant improvements in segmentation accuracy when compared to multi-scale GVF (MGVF) and multi-scale VFC (MVFC).

2. MULTI-SCALE TENSOR VECTOR FIELD

In MTVF, a given image I_0 is downsampled repeatedly for n iterations based on some constant ratio $r(0 < r < 1)$ to construct a set of downsampled images $I_\iota \forall \iota \in \mathbb{Z}[0, n]$ with I_n denoting the image at the lowest scale. A contour c_0 is then initialized either manually or automatically for given image I_0 and rescaled by r^n to construct a contour c_n for I_n. Starting at scale n, for a scale ι, the initial contour c_ι is used to obtain a final contour $\hat{c_\iota}$ by minimizing the energy at that scale. $\hat{c_\iota}$ is rescaled by $1/r$ to obtain $c_{\iota-1}$, which acts as the initial contour for scale $\iota - 1$. This process is repeated until the energy is minimized at scale I_0.

At scale ι, the initial contour c_ι is expressed in terms of its arc length s as $c_\iota(s) = (x(s), y(s)) \forall s \in [0, 1]$, where $x(s)$ and $y(s)$ are the co-ordinates of c in terms of s. The energy of c_ι, $E_{AC,\iota}$ is expressed as,

$$E_{AC,\iota} = \int_0^1 \Big[E_{int,\iota}\big(c_\iota(s)\big) + E_{ext,\iota}\big(c_\iota(s)\big)\Big] ds \quad (1)$$

where $E_{int,\iota}$ is the internal energy and $E_{ext,\iota}$ is the external energy of c_ι. The final contour $\hat{c_\iota}$ is obtained by iteratively minimizing $E_{AC,\iota}$. $E_{int,\iota}$ is usually expressed in terms of first and second derivatives of the contour to limit discontinuities and sharp changes along c_ι, and can be expressed as

$$E_{int,\iota} = \frac{1}{2}(\alpha|c'_\iota(s)|^2 + \beta|c''_\iota(s)|^2)$$

where constants α and β control the relative weights of the first and second derivative constraints. $E_{ext,\iota}$ forces c_ι towards the object boundary, and as such capture range and noise sensitivity are mainly decided by $E_{ext,\iota}$. $E_{AC,\iota}$ is minimized by iteratively solving Eq. (2), which is obtained by differentiating Eq. (1) with respect to s_ι:

$$\underbrace{\alpha c''_\iota(s) - \beta c''''_\iota(s)}_{F_{int,\iota}} - \underbrace{\Delta E_{ext,\iota}}_{-F_{ext,\iota}} = 0 \quad (2)$$

The $F_{ext,\iota}$ at each scale is computed via the tensor vector field at ι, and will be described in the next subsection.

2.1. Tensor Vector Field Computation

The tensor vector field at scale ι is obtained by convolving the edge map f_ι with the adaptive kernel $\mathbf{k}_\iota$ of size $a \times a$, where a decides the capture range of the contour. Let $\mathbf{n}(i, j)$ and $m(i, j)$ denote the unit vector towards the center of the kernel and the magnitude of those vectors respectively at position (i, j). $m(i, j)$ is reduced as a function of the distance from the center of the kernel. The function is given as $m(i, j) = (r + \epsilon)^{-\zeta}$, where $r = \sqrt{i^2 + j^2}$, and ζ is constant. The adaptive kernel $\mathbf{k}_\iota$ is computed by utilizing the structural information contained in the object boundary at a given scale ι. A weighted image tensor Γ_ι [9] can be expressed as,

$$\Gamma_\iota(x, y) = \begin{pmatrix} \sigma_{x,x} & \sigma_{x,y} \\ \sigma_{y,x} & \sigma_{y,y} \end{pmatrix} \quad (3)$$

where $\sigma_{x,x}$, $\sigma_{y,y}$ are weighted variance and $\sigma_{x,y}$ is weighted covariance of image gradients $u_{x,\iota}$ and $u_{y,\iota}$ along x and y respectively. A Gaussian kernel $\mathbf{g}$ of size $\kappa \times \kappa$ is used to compute $\sigma_{x,x}$, $\sigma_{y,y}$, and $\sigma_{x,y}$ as,

$$\sigma_{x,y} = \sum_{i=-\kappa/2}^{\kappa/2} \sum_{j=-\kappa/2}^{\kappa/2} g(i, j) u_x(i, j) u_y(i, j)$$

where $g(i, j)$ is an element of the $\mathbf{g}$ at (i, j). $\sigma_{x,x}$ and $\sigma_{y,y}$ are computed in similar way. $\Gamma_\iota(x, y)$ gives the variation of gradients at position (x, y) for I_ι. Eigenvalue decomposition is done on Γ_ι at each pixel. The major eigenvector $\mathbf{v}_{+,\iota}(x, y)$ corresponding to maximum eigenvalue $\lambda_{+,\iota}(x, y)$ gives the direction along maximum gradient at position (x, y).

During convolution of $\mathbf{k}_\iota$ with edge-map f_ι, for each position (i, j) of k on f, the kernel is modified based on $\lambda_{+,\iota}(i, j)$ and $\mathbf{v}_{+,\iota}(i, j)$. Each kernel vector $\mathbf{k}(i, j)$ is adapted to change its magnitude based on the projection length of $\mathbf{v}_{+,\iota}(i, j)$ on $\mathbf{k}(i, j)$, so $\mathbf{k}(i, j)$ remains unchanged if it is along $\mathbf{v}_{+,\iota}(i, j)$,

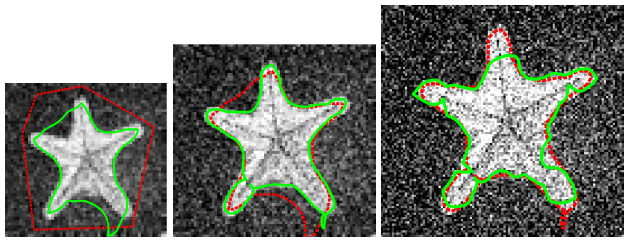

(a) $MGVF_2$ (b) $MGVF_1$ (c) $MGVF_0$

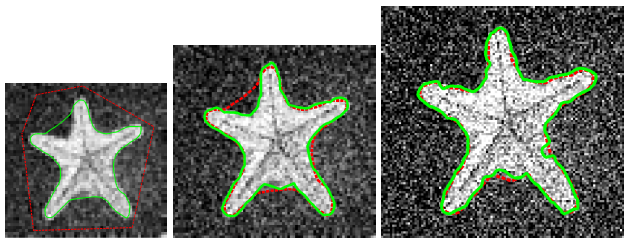

(d) $MTVF_2$ (e) $MTVF_1$ (f) $MTVF_0$

Figure 3: Intermediate convergence results for noisy starfish image Fig. 2a for MGVF and MTVF after 5 iterations. Red curve: initial contour, green curve: final contour.

and $\mathbf{k}(i,j)$ sets to zero if it is perpendicular to $\mathbf{v}_{+,\iota}(i,j)$. Hence, the adaptive kernel $\mathbf{k}_\iota$ at each point (i,j) can be expressed as,

$$\mathbf{k}_\iota(i,j) = |\mathbf{n}(i,j) \cdot \mathbf{v}_+(i,j)|\lambda_+(i,j)\mathbf{n}(i,j). \qquad (4)$$

Finally, the TVF at scale ι is obtained by normalizing the convolution result at each pixel.

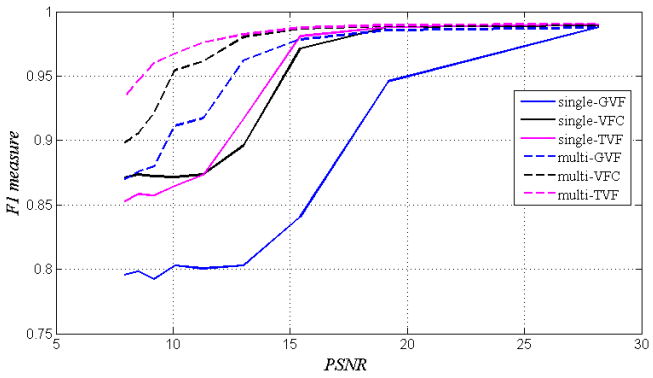

Figure 4: A comparison of the F1-measure for six active contour methods for a range of PSNR. The multi-scale approaches outperform their single-scale counterparts, with MTVF providing the best results for all cases.

3. RESULTS AND ANALYSIS

We have tested three methods — GVF, VFC, TVF — and their multiscale counterparts MGVF, MVFC, and MTVF. For

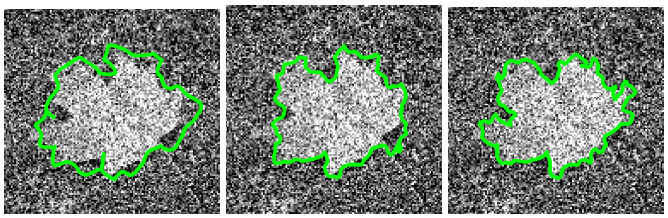

(a) MGVF (b) MVFC (c) MTVF

Figure 5: Segmentation results for a maple leaf image contaminated with Gaussian noise at 12.3 dB.

each case, the same initial contour and same edge maps at each resolution level ι were used. For the single scale methods we kept their parameters the same as suggested in their original papers: Kernel size ($a = 65$), mask size ($\kappa = 5$), $\zeta = 2.8$, and the standard deviation of the Gaussian kernel $\mathbf{g} = 1$. n can effect results in following way,

- Very high n can make objects of interest very small. For very small objects, in the absence of proper opposing external field inside object the active contour can shrink significantly or even collapse to one point.
- At the coarsest level I_n, the contrast across object boundary can reduce significantly and the presence of high noise aggravates blurring problem.

Images are downsampled by $r = 1/\sqrt{2}$ for two times $n = 2$ for 100×100 images, while n is kept 3 for 300×200 samples. The single scale methods were performed for 30 iterations, while 5 iterations was performed per scale for the multi-scale methods. For MVFC and MTVF, the kernel size (a) is set to half of the lowest scale resolution and is kept constant for all finer scales, as the initial contour reaches quite close to the object boundary at coarser scales and after that we do not require large a for high capture range.

For quantitative comparison purposes, the F1-measure [10] was computed, given its wide use in the active contour literature. The measure ranges from 0 (worst) to 1 (best). Gaussian noise at different standard deviations was added to the test images to simulate high noise conditions. Tests for each case have been repeated 20 times by independently adding noise to obtain consistent results.

Figs. 1 compare results for the starfish image at 14.2 dB for GVF, MGVF, and TVF. It can be observed that MTVF (Fig. 3f) outperforms the other methods in terms of capturing the irregular boundary of the starfish object. In particular, Fig. 2 shows the streamlines of MTVF at different scales, which show how a point will move at a given scale under the influence of the external field. A higher density and a consistency towards the image boundaries ensures better convergence of active contour. At the coarsest level I_2, the scale at which we wish to obtain a large capture range, we can see that MTVF remains un-influenced by noise; for the finest

(a) Starfish (b) Brain (c) Tank (d) Snail (e) Maple (f) B.fly

Figure 6: Sample test images. Figs. (a-d), approx. size 100×100. Figs. (e,f), approx. size 300×200.

Image	PSNR	F_1 measure					
		GVF	MGVF	VFC	MVFC	TVF	MTVF
Starfish	10.6	0.82	0.92	0.89	0.95	0.90	**0.96**
Brain	10.8	0.90	0.96	0.93	0.96	0.95	**0.97**
Tank	12.9	0.93	0.96	0.93	0.96	0.94	**0.97**
Snail	12.9	0.92	0.94	0.92	0.95	0.92	**0.96**
Maple	13.3	0.89	0.95	0.89	0.96	0.90	**0.98**
B.fly	14.8	0.92	0.95	0.93	0.97	0.93	**0.98**

Table 1: A comparison of F_1 measure (mean of 20 repetitions) for sample test images (Fig. 6) contaminated with Gaussian noise.

scale I_0, though there is significant noise influence, MTVF remains consistent near the object boundaries, which helps in minimizing distraction for the closely converged contour from coarser scales. In Fig. 3 we have shown the final position of the active contour at each level ι after 5 iterations for MGVF and MVFC.

In Fig. 4 the performance trend is shown for the compared methods in terms of the F1-measure as a function of noise level. We can see, in all cases, that the multi-scale methods provide improved segmentation accuracy compared to their single-scale counterparts. It can also be observed that MTVF outperforms and remains consistent for very high noise levels compared to all other methods. Further, Table 1 shows that MTVF noticeably outperforms all other tested methods for each tested image at high noise levels, convincingly illustrating the noise robustness of the proposed MTVF method. An example segmentation using the tested methods for the noisy maple leaf image at 12.3 dB is shown in Fig. 5, again showing that MTVF provides noticeably improved segmentation results compared to the other methods.

4. CONCLUSION

In this paper we have presented a novel multi-scale TVF (MTVF) based active contour. The results of MTVF have been compared with multi-scale GVF (MGVF) and multi-scale VFC (MVFC). Through experiments on standard sample images under high noise levels, it has been shown that MTVF consistently performs better compared to other state-of-the art counterparts. Future work involves investigating alternative scale decomposition methods as well as incorporating additional image information into the external energy function.

Acknowledgment

We would like to thank authors of [7] for providing very useful the VFC code, which helped us in generating comparative results.

5. REFERENCES

[1] M. Kass, A. Witkin, and D. Terzopoulos, "A snakes-active contour models," *International Journal of Comp. Vision*, vol. 1, pp. 321–331, 1987.

[2] C. Xu and J. L. Prince, "Generalized gradient vector flow external forces for active contours," *Signal Processing*, vol. 71, pp. 131–139, December 1998.

[3] H. Yu, L. Li, W. Xu, W. Liu, J. Zhang, and G. Shao, "Gaussian pyramid based multi-scale GVF snake for mass segmentation in digitized mammograms," in *Proc. International Conf. on Bioinfo. and Biomed. Eng., 2009*, June 2009, pp. 1–4.

[4] A. Kumar, A. Wong, A. Mishra, D. A. Clausi, and Paul Fieguth, "Tensor vector field based active contours," in *Proc. International Conf. on Image Processing, 2011*, 2011.

[5] F. Shih and K. Zhang, "Locating object contours in complex background using improved snakes," *Computer Vision Graphics and Image Understanding*, vol. 105, pp. 93–98, 2007.

[6] A. Jalba, M. Wilkinson, and J. Roerdink, "CPM: A deformable model for shape recovery and segmentation based on charged particles," *IEEE Trans. Pattern Anal. Mach. Intell.*, vol. 26, pp. 1320–1335, October 2004.

[7] B. Li and S.T. Acton, "Active contour external force using vector field convolution for image segmentation," *IEEE Trans. Image Process*, vol. 16, pp. 2096–2106, August 2007.

[8] B. Leroy, I. Herlin, and L. Cohen, "Multi-resolution algorithms for active contour models," in *ICAOS '96*, vol. 219, pp. 58–65. Springer Berlin / Heidelberg, 1996.

[9] R. L. Deluisgarcia, R. Deriche, and C. A. Lopez, "Texture and color segmentation based on the combined use of the structure tensor and the image components," *Signal Processing*, vol. 88, pp. 776–795, April 2011.

[10] A. K. Mishra, P. W. Fieguth, and D. A. Clausi, "Decoupled active contour (dac) for boundary detection," *IEEE Trans. on Pattern Anal. Mach. Intell.*, vol. 33, pp. 310–324, 2011.